International Journal of Science and Research (IJSR)
ISSN (Online): 2319-7064
Index Copernicus Value (2013): 6.14 | Impact Factor (2013): 4.438

Structural and Dielectric Investigations on $x[Ba_{0.7}Ca_{0.3}TiO_3]$-$(1-x)[BaZr_{0.2}Ti_{0.8}O_3]$ Lead-Free Mixed Ceramic Compositions

S.S. Mane[1], D.J. Salunkhe[2]

[1]Nano-composite laboratory, Karmaveer Bhaurao Patil Mahavidyalaya, Pandharpur, Solapur, 413304, India
[2]Nano-composite laboratory, Karmaveer Bhaurao Patil Mahavidyalaya, Pandharpur, Solapur, 413304, India

Abstract - ***Lead-free nanopowders of $Ba_{0.7}Ca_{0.3}TiO_3$(BCT) and $BaZr_{0.2}Ti_{0.8}O_3$ (BZT) were prepared using a solid-state reaction technique. The nanoparticles are used to form composites xBCT-(1-x)BZT for x = 0.40, 0.45 and 0.50 with 2wt% Bi_2O_3 as a sintering aid. The structural, microstructural, dielectric properties and polarisation of the composites have been investigated and discussed. All the samples possess pure perovskite structure. The result on variation of dielectric constant with temperature and frequency are promising and suggest usefulness of composites as a RF dielectric material, in paraelectric region. The investigations on the P-E hysteresis loop reveal that all the compositions possess useful values of maximum polarization (Pmax) and remnant polarization (Pr). The present observations suggest that, the xBCT-(1-x)BZT could be a useful ferroelectric system.***

Keywords: Composites, Solid-state reaction, Microstructure, Dielectric properties.

1. Introduction

Perovskite oxides derived from $BaTiO_3$ are well known for their applications as materials in electronics, pulse generating devices, transducers, infrared detectors etc. Amongst these materials, pure and substituted $BaTiO_3$ (BT) presents excellent dielectric and piezoelectric properties. Lead based ferroelectric ceramics have been at the forefront of ceramic industry since decades. This is due to their excellent dielectric, piezoelectric properties and electromechanical coupling coefficients. So far, lead zirconate titanate (PZT) was the most widely used piezoelectric materials due to their excellent piezoelectric properties in the vicinity of the morphotropic phase boundary (MPB) between rhombohedral and tetragonal phases [1],[2],[3],[4],[5],[6]. Nevertheless, they are not environment friendly for lead oxide toxicity. With the recent growing demand of global environmental protection, many researchers have greatly focused on lead-free ceramics to replace the lead based ceramics [7],[8],[9], [10]. Recently, the focus of study is on lead free ferroelectric ceramics. Liu et al. first reported a lead free pseudo-binary $x[(Ba_{0.7}Ca_{0.3})TiO_3]$-$(1-x)[Ba(Zr_{0.2}Ti_{0.8})O_3]$ (BCT-BZT) (hereafter abbreviated as xBCT-(1-x)BZT) ferroelectric system to replace lead zirconate titanate (PZT) based systems[7]. This system possesses a MPB near 50-50 composition similar to PZT system and it exhibits an equally excellent piezoelectricity as in Pb-based systems [7]. BT is known to have a large electromechanical coupling coefficient. Substitution of Ti^{4+} (ionic radius of 74.5 pm) with Zr^{4+} (atomic radius of 86 pm) exhibits several interesting features in the dielectric behaviour of BT ceramics. When the Zr content less than 10% in $BaZr_xTi$ $(1-x)O_3$ (BZT) ceramics show normal ferroelectric behaviour and the dielectric anomalies corresponding to the cubic to tetragonal (Tc), tetragonal to orthorhombic (T2) and orthorhombic to rhombohedra l(T3) phases have been clearly observed [8], [9].The modified BZT has shown the systematic changes in dielectric, piezoelectric and phase transition characteristics in bulk ceramic and single crystal form [10], [11].

Recently Xue et al. reported dielectric and piezoelectric properties of a lead free morphotropic phase boundary (MPB) of composition 0.5BCT-0.5BZT [8]. The newly reported BZT-xBCT system exhibits very high piezoelectric performance. For the MPB composition (50BCT-50BZT), the piezoelectric coefficient d_{33} is found to be a very high value of 580-600 pC/N [8],[9]. The related system of (BCT-BZT) ceramics is reported to exhibit a broad dielectric constant-temperature curve near Tc with value as high as 17000 [12]. The BZT ceramics with various grain sizes showed a relaxor ferroelectric behavior, which follows the Vogel-Fulcher relation [13].These ceramics are promising materials for tunable capacitor applications. Owing to discussion above, the present paper report synthesis and characterization of BCT, BZT and compositions xBCT-(1-x)BZT for x = 0.40, 0.45 and 0.50. The paper reports analysis of crystal structure, the observed microstructure, dielectric constant as a function of temperature and frequency, dielectric loss as a function of temperature at frequency f=1kHz, diffusivity parameter (γ), diffuseness parameter(δ), Vogel-Fulcher Relation and ferroelectric hysteresis loops of BCT, BZT and compositions xBCT-(1-x)BZT for x = 0.40, 0.45 and 0.50.

2. Experimental

The individual phases of BCT and BZT were prepared by the conventional ceramic method. The AR grade starting materials with high purity (>99.9%) $BaCO_3$, CaO, ZrO_2, and TiO_2 were taken in the required stoichiometric ratio and milled for 3 hours in an agate mortar [10]. The milled powders were pre-sintered at 1100°C for 12hours. These powders were uniaxially pressed in a die to form pellets (thickness of 1-2 mm and diameter of 1.2 cm) using hydraulic press. Polyvinyl alcohol (10% of its weight) was used as a binder during the formation of pellets. The resulting

powders with pellets were final sintered at1200°C for 12 hours at the rate of 1 °C/min and natural cooling was adopted for the both heat treatments. Different compositions of BCT and BZT as 0.40BCT-0.6 0BZT, 0.45BCT-0.55BZT and 0.50BCT-O.50BZT were prepared by same ceramic method and sintered at1200°C for 12 hours. In the present case, the silver paint was employed as an electrode for characterization, where it is observed that by using silver paint the electrode effect could be minimized [14].

The parent phase BCT and BZT as well as their compositions $x[Ba_{0.7}Ca_{0.3}TiO_3]$-(1-x)$[BaZr_{0.2}Ti_{0.8}O_3]$ were investigated for the structural properties using X-ray powder Diffractometer (Bruker D8 XRD spectrometer has been used) . SEM images of calcined powders were obtained using JEOL-JSM 6360 SEM scanning electron microscope. For dielectric measurements LCR-Q meter (HP4284A) was used in the frequency range from 100 Hz to 1 MHz and temperature T between room temperature to 160 °C. The P-E measurements of BCT, BZT and xBCT-(1-x)BZT samples at 50 Hz were carried out using P-E loop tracer model no.609B Radient Technologies, USA (UGC-DAE-CSR, Indore (India).

3. Results and discussion

3.1 Structural Analysis

The individual powders of the BCT and BZT are investigated for structural studies for confirmation of formation of the desired phase and estimation of the particle size. Fig. 1 shows the XRD patterns of the $Ba_{0.7}Ca_{0.3}TiO_3$ (BCT) ceramics.

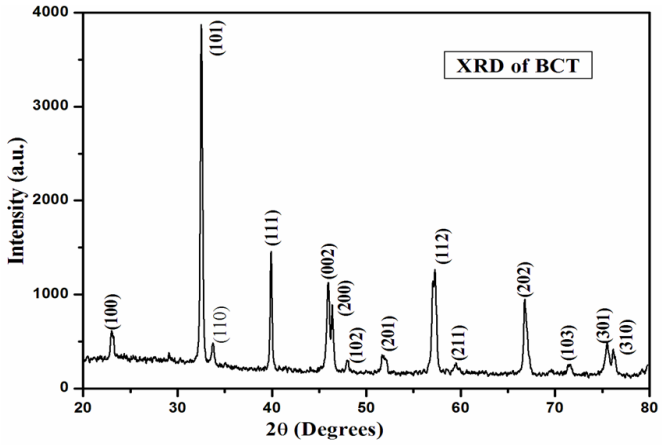

Figure 1: XRD of BCT

As can be seen, the sample shows pure perovskite structure, suggesting that Ca diffuse into the $BaTiO_3$ lattice to form a solid solution. The reflections are in confirmation with the JCPDS data on $BaTiO_3$ possessing perovskite crystal structure. The lattice parameters 'a' and 'c' are observed to be $3.982A^0$and $4.020A^0$ respectively, which is in confirmation with earlier reports. This process has led to the formation of BCT phase of particles size nearly 44nm as determined from the XRD spectra using Scherrer formula [15]. Fig.2 shows the XRD patterns of the $BaZr_{0.2}Ti_{0.8}O_3$ (BZT) ceramics. As can be seen, the sample shows pure perovskite structure, suggesting that Zr diffuse into the $BaTiO_3$ lattice to form a solid solution which too shows the reflections corresponding to perovskite crystal structure is in confirmation with the earlier reports [15],[16],[17].

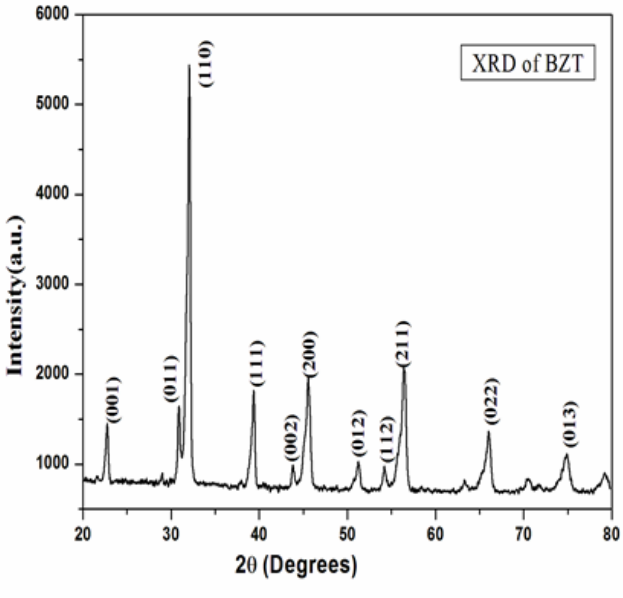

Figure 2: XRD of BZT

The particle size of BZT is observed to be 23nm as determined using Scherrer formula. The parameters 'a' and 'c' determined from the XRD spectra are a = b = $4.055A^0$ and c = $4.212A^o$.From XRD spectra it is observed that BCT and BZT have tetragonal crystal structure.

Fig. 3 presents the XRD pattern of the sintered xBCT-(1-x) BZT ceramic. The sample exhibits perovskite structure with no trace of impurity, suggesting that Ca and Zr diffuse into the $BaTiO_3$ lattice to form a homogeneous solid solution.

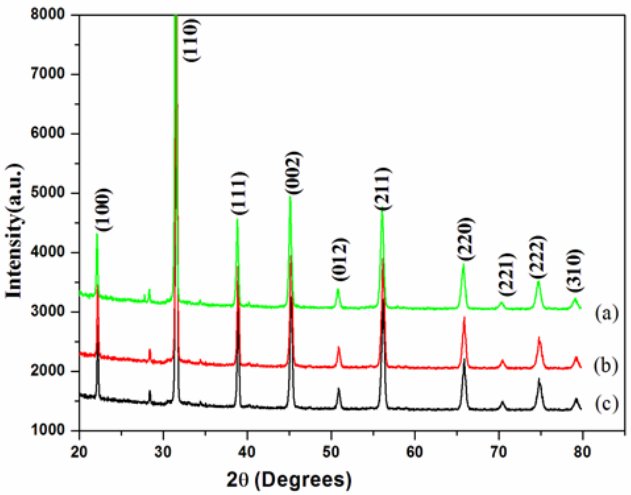

Figure 3: XRD of (a) (0.50BCT-0.50BZT) (b) (0.45BCT-0.55BZT) (c) (0.40BCT-0.60BZT

It could be seen that the composite materials grown are polycrystalline in nature. While the compositions of (x) BCT- (1-x) BZT for x= 0.40, 0.45 and 0.50 have mild tetragonal nature at room temperature [18]. Table 1 shows the lattice parameter a, c, c/a ratio and average particle size of parent and each composite material. The average particle size (D) is calculated using Scherrer's formula i.e.

$D = K*\lambda/(\beta *Cos\theta)$

Where the k is constant having value 0.9, λ is wavelength of Cu kα line of XRD target, β is full width at half maxima and

θ is the angle of diffraction.

We did not detect any reflection corresponding to any impurity phase in the XRD spectra, suggesting the single phase growth of the composite material.

Table 1: The lattice parameter a, c, ratio c/a and average particle size (D)

Composition	a (Å)	c (Å)	c/a	D (nm)
BCT	3.982	4.020	1.009	44
BZT	4.055	4.212	1.038	23
0.40BCT-0.60BZT	3.974	4.017	1.010	33
0.45BCT-o.55BZT	4.006	4.529	1.130	40
0.50BCT- 0.50BZT	4.009	4.014	1.001	31

Thus from the analysis of XRD it appears that the nano-composite materials are formed in the desired crystal structures.

3.2 Micro-structural analysis

SEM pictures are obtained using JEOL-JSM 6360 SEM. Fig.4 (a), (b), (c) and (d) show the SEM images with resolution 5000 of pellet samples of BCT, BZT, 0.4BCT-0.6BZT, and 0.5BCT-0.5BZT compositions respectively.

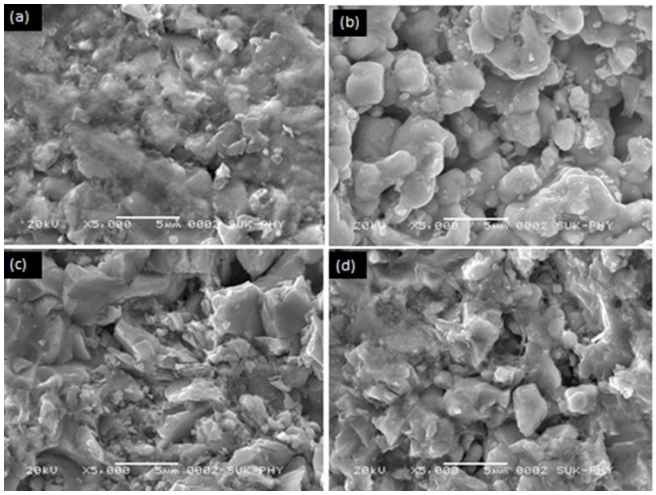

Figure 4: SEM of (a) BCT (b) BZT (c) 0.40BCT- 0.60BZT (d) 0.50BCT-0.50BZT

From SEM images it is seen that the samples are compact microstructure and with some voids are seen in the SEM images. The observed average grain size from SEM image is nearly 2µm. It could be seen from the figure that, the microstructure of the material is fairly uniform and the samples appeared to be fairly dense.

3.3 Dielectric Properties

Fig.5 shows the temperature dependent dielectric constant of 0.40BCT-0.60BZT composition at various frequencies ranging from 100 Hz to 1MHz. Here the dielectric constant ε is determined relative to the dielectric constant of the free space. It is observed that the ε passes through a peak at the Curie temperature T_c. Additionally it could be seen from the fig.5 that the T_c shifts slightly towards higher temperature as the frequency increases from 100 Hz to 1 MHz.

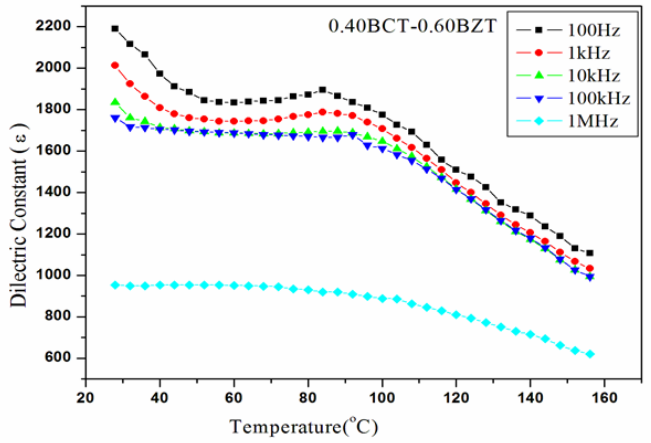

Figure 5: The dielectric constant of 0.40BCT-0.60BZT ceramics as a function of measuring temperature and frequency.

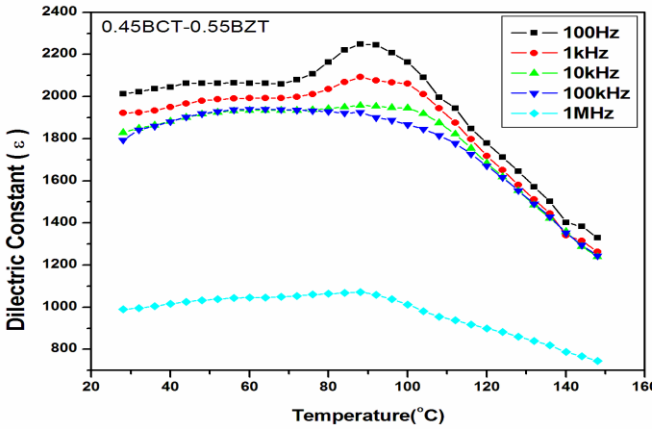

Figure 6: The dielectric constant of 0.45BCT-0.55BZT ceramics as a function of measuring temperature and frequency.

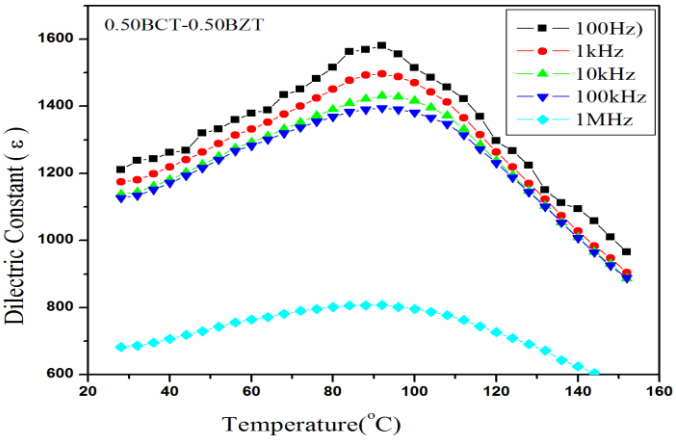

Figure 7: The dielectric constant of 0.50BCT-0.50BZT ceramics as a function of measuring temperature and frequency.

Moreover, the dielectric constant shows only slight frequency dependence. These results are consistent well with those previously reported [7]. Further, it appears that the transition is a diffused phase transition (DPT). These features indicate that the 0.40BCT-0.60BZT is DPT material having a signature of relaxor behaviour [19].Table 2 shows Curie temperature (T_c), maximum dielectric constant (ε_{max}), loss

tangent at T_c (tan δ_{Tc}), diffusivity (γ) and diffusion parameter (δ) at T_c for various frequencies for the 0.40BCT-0.60BZT composition.

Table 2: Variation of ε, tan δ, Tc, γ and δ with frequency for 0.40BCT+0.60BZT

Frequency	T_c °C	ε_{max}	tan δ_{Tc}	γ	$\delta*10^{-5}$
100 Hz	84	1884.30	0.02857	1.69	2.89
1 kHz	84	1787.15	0.03649	1.74	2.77
10 kHz	85.4	1696.29	0.03344	1.22	2.75
100 kHz	86	1648.78	0.02994	1.56	5.08
1 MHz	86.2	920.35	0.30674	1.76	3.69

Table 3: Variation of ε, tan δ, Tc, γ and δ with frequency for 0.45BCT+055BZT

Frequency	T_c °C	ε_{max}	tan δ_{Tc}	γ	$\delta*10^{-5}$
100 Hz	88	2248.37	0.0438	1.814	1.434
1 kHz	88	2092.91	0.0492	1.819	4.374
10 kHz	89.3	1957.60	0.0413	1.977	2.684
100 kHz	89.9	1914.42	0.0341	1.302	2.139
1 MHz	90	1072.13	0.3174	1.568	2.872

Table 4: Variation of ε, tan δ, Tc, γ and δ with frequency for 0.50CT+0.50BZT

Frequency	T_c °C	ε_{max}	tan δ_{Tc}	γ	$\delta*10^{-5}$
100 Hz	91.92	1580.48	0.0262	1.355	4.950
1 kHz	92	1496.99	0.0321	1.741	2.805
10 kHz	92.3	1430.78	0.0321	2.137	1.732
100 kHz	92.61	1394.79	0.0319	1.989	2.006
1 MHz	93	808.07	0.2717	1.292	4.322

Fig.6 and Fig.7 show variation of ε as a function of temperature at various frequencies ranging from 100 Hz to 1MHz for the composites 0.45BCT-0.55BZT and 0.50BCT-0.50BZT respectively. Determined values of γ and δ are shown in Table 3 and Table 4 respectively. From these tables it observed that in case of these two compositions also the γ is between 1 and 2 indicating a partial relaxor behavior. Further, these composites show the transitions to be a diffuse phase transitions (DPT) [12], [18].

In case of (BCT-BZT) composition Ca is substituted at A site, while Zr is substituted at B site of ABO_3 of ferroelectric system, more than one cataion A and B site may lead to various local region of different relaxation time [20]. These polar micro domains are responsible for the observed relaxor behavior. To parameterize this observe variation of ε versus T behavior, the ε in the paraelectric region is fitted to an equation called modified Curie-Weiss law [21], [22], [23].

$$\frac{1}{\varepsilon} = \frac{1}{\varepsilon_{max}} + \frac{(T - T_c)^{\gamma}}{2\delta^2 \varepsilon_{max}} \quad \ldots\ldots\ldots\ldots 1$$

Here γ is diffusivity and δ is diffusion parameter.

Graph between ln (1/ ε - 1/ ε_{max}) and ln (T-Tc) is linear (Fig. 8).

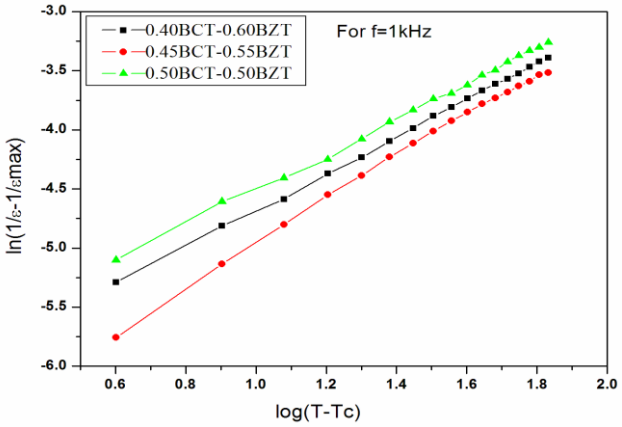

Figure 8: Variation of ln(1/ε-1/εmax) versus ln(T-T_c) for xBCT-(1-x)BZT ceramics for x= 0.40, 0.45, 0.50 at frequency f=1kHz.

The slope of the fitting curves is used to determine the γ value and intercept is used to determine δ value. γ is ranging from 1(a normal ferroelectric) to 2 (an ideal relaxor ferroelectric). Determined values of γ and δ are shown in Table 3, Table 4 and Table 5. These observations suggest that compositions possess a diffuse phase transition characteristics of a relaxor material.

In relaxor materials, an empirical Vogel–Fulcher (VF) relationship can be used to account for the dielectric relaxation nature. The dielectric relaxation appears as a result from thermally activated polarization between two equivalent variants. Based on this model, the polarization flipping frequency f_0 (the operating frequency) is related to the activation energy Ea (the barrier between two equivalent polarization states). To confirm to existence of relaxor contribution, variation of T_c as function of frequency has been fitted to an equation [22].

$$f = f_0 \, exp\left[\frac{-E_a}{K_B(T_c - T_f)}\right] \quad \ldots\ldots\ldots 2$$

Where f, f_0, K_B and E_a are the operating frequency, pre-exponential factor, Boltzmann Constant and the activation energy respectively, while T_f is the freezing temperature. T_f is regarded as the temperature where the dynamic reorientation of the dipolar cluster polarization can no longer be thermally activated. For the purpose of confirmation that the variation of T_c with frequency f obeys the Vogel-Fulchar relation, a graph of variation of ln(f) verses 1000/Tc is plotted and shown in Fig.9 for for xBCT-(1-x)BZT ceramics for x= 0.40, 0.45, 0.50.

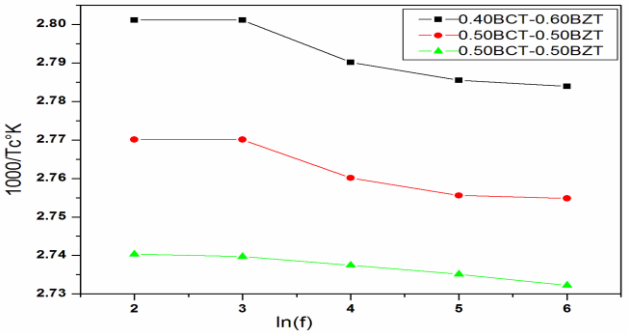

Figure 9: Verifying Vogel-Fulcher Relation for xBCT-(1-x)BZT ceramics for x= 0.40, 0.45, 0.50

The variation of ln(f) with 1000/Tc is non-linear as required for a relaxor material.

Fig. 10 shows variation of tangent loss (δ) factor of xBCT-(1-x)BZT ceramics for x= 0.40, 0.45, 0.50 as a function of measuring temperature at frequency f=1kHz. The curves were obtained on heating of the samples.

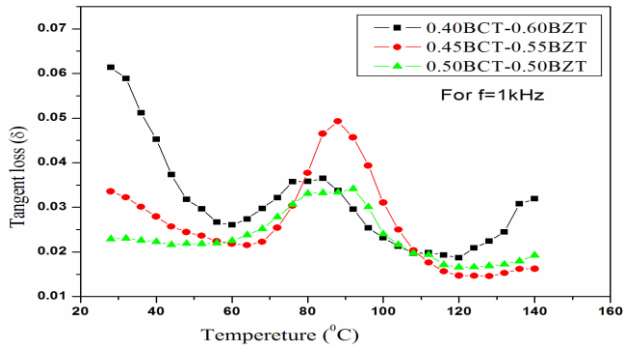

Figure 10: Variation of tangent loss (δ) factor ofxBCT-(1-x)BZT ceramics for x= 0.40, 0.45, and 0.50 as a function of measuring temperature at frequency f=1kHz.

The maxima of the tanδ obtained at T_c. As x increases T_c increases. Higher losses are observed for the 0.45BCT-0.55BZT sample, while lower losses are seen for 0.50BCT-0.50BZT sample as compare to other compositions at T**c** **[**11], [21].

3.4 P-E Hysteresis of compositions

Fig.11 shows a typical *P-E* hysteresis loop for each BCT, BZT, 0.4BCT-0.6BZT, 0.45BCT-0.55BZT and 0.5 BCT-0.5BZT nano-composites. The observed values of saturation polarization P_{max}, remnant polarization P_r , the coercive electric field E_c and the ratio P_r/P_{max} for parent and composites obtained from the *P-E* hysteresis loops are given in the Table 5. A significant change in electric polarization, remnant polarization and coercive electric force is observed. From the ferroelectric polarization studies it is seen that the composition 0.5BCT-0.5BZT have maximum value of P_s (5.6μC/Cm^2) and P_r (1.57μC/Cm$^{2)}$ as compared to other compositions at room temperature[12][24][25].

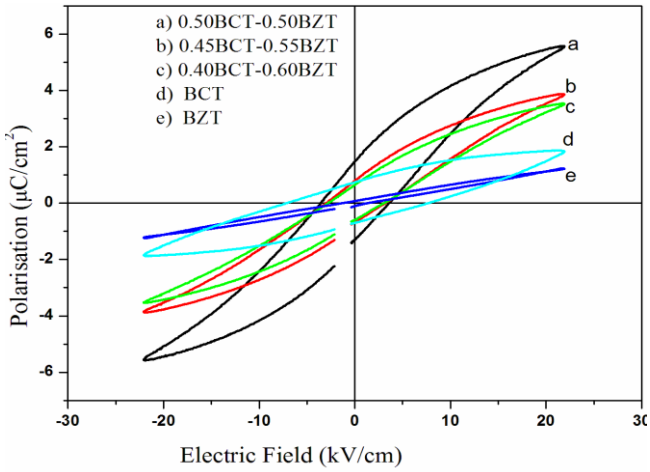

Figure 11: P-E hysteresis loops for a) 0.50BCT-0.50BZT b) 0.45BCT-0.55BZT c) 0.40BCT-0.6BZT d) BCT e) BZT

Table 5: Observed values of Ps, Pr, and Ec.

Composition	P_{max} (μC/Cm^2)	P_r (μC/Cm^2)	E_c(kV/Cm)	P_r/P_{max}
BCT	1.892	0.803	5.271	0.424
BZT	1.294	0.204	1.894	0.157
BZT-0.4BCT	3.491	0.661	2.143	0.190
BZT-0.45BCT	3.987	0.748	2.261	0.187
BZT-0.5BCT	5.602	1.575	3.612	0.281

4. Conclusions

From the XRD analysis it is observed that the BCT, BZT and xBCT-(1-x) BZT nano-composites are polycrystalline, phase pure, with tetragonal crystal structure. From SEM it is observed that a homogeneous microstructure with grain size around 2μm is observed. Temperature dependence dielectric constant shows, it is maximum at T_c. From the dielectric studies with temperature, it is observed that the Curie temperature T_c and the ferroelectric to paraelectric phase transition occur at 84°C, 86°C and 92°C for 0.4BCT-0.6BZT, 0.45BCT-0.55BZT and 0.5 BCT-0.5BZT systems respectively. Additionally the composites show a relaxor behavior. Dielectric loss is Maximum at T_c for each composite. Loss is Minimum for 0.5BCT-0.5BZT system as compare to other systems at T_c. From the ferroelectric polarization studies it is seen that the composite 0.5BCT-0.5BZT have maximum value of P_s (5.6μC/Cm^2) and P_r(1.57μC/Cm$^{2)}$ as compared to other composites at room temperature. All the compositions are observed to possess a significant value of P_r/P_{max}.

5. Acknowledgements

Authors are thankful to DRDO-NRB, New Delhi (India) for their financial support and also UGC-DAE-CSR, Indore (India) to carry out the P-E Hysteresis loops.

References

[1] M. R. Soares, A. M. R. Senos, and P. Q. Mantas, Journal of the European Ceramic Society, v 20 (3) (2000) pp 321– 334.
[2] H.Tabatay, Y.Hottaand T.Kawai Journal of the Korean Physical Society, 42 (2003) S1199-S1202.
[3] B. K.Gan and K. Yao, Ceramics International, 35 (5) (2009) pp2061–2067.
[4] P. Kumar, S. Sharma, O.P. Thakur, C.Prakash, and T. C. Goel, Ceramics International, 30 (4) (2004) pp585– 589.
[5] D. Zhou, Y. Tang, F. Wang et al., Thin Solid Films, 522 (2012) pp 457–462.
[6] M. Roth, E. Dul'In, E. Mojaev, and M .Tseitlin, Optical Materials, 34(2) (2011)pp 381–385.
[7] W. Liu and X. Ren, Physical Review Letters, 103 (ID 257602) (2009) pp. 1–4.
[8] D. Xen, Y Zhou, H. Bao, C Zhou, J. Gao and X. Ren, Journal of Applied Physics 109 (2011) 054110.
[9] J. Gao, D Xue, Y. Wang, D Wang, L Zhang, H Wu, S Guo, H Bao, C Zhou, W. Liu, S Hou, G. Xiao, and X. Ren, Applied Physics Letters 99 (2011) 092901.
[10] D. Damjanovic, A. Biancoli, L. Batooli, A. Vahabzadeh, and Joe Trodahl Applied Physics Letters 100 (2012) 92907.

[11] C. E. Ciomaga, R. Calderone, M. T. Buscaglia, M. Viviani,V. Buscaglia, L. Mitoseriu, A. Stancu, P. Nanni, Journal of Optoelectronics and Advanced Materials 8(3) (2006) p. 944 – 948.
[12] Shi Su, R Zuo , S. Lu , Z. Xu , X. Wang , L.Li, Current Applied Physics 11 (2011) S120-S123.
[13] C. Fu, F. Pan, W. Cai, and X. Deng, Integrated Ferroelectrics, 104 (2008) p1–7.
[14] S. R. Jigajeni, A. N. Tarale, D. J. Salunkhe, P. B. Joshi, S. B. Kulkarni, Ceramics International 39 (2013) 2331.
[15] F. Mouraa, A. Z. Sim˜oes , B. D. Stojanovic, M. A. Zaghete , E. Longoa, J. A. Varela, Journal of Alloys and Compounds 462 (2008) 129–134
[16] W. Li, Z. Xu, R. Chu, P. Fu, and G. Zang, Brazilian Journal of Physics, 40(3) (2010).
[17] F. Moura, A. Z. Simões, .C A. Paskocimas, M. A. Zaghete, J. A. Varela, E. L.ongo Materials Chemistry and Physics 123 (2010) 772–775.
[18] I. Coondoo, N. Panwar, H. Amorın, M. Alguero, and A. L. Kholkin, Journal of Applied Physics 113 (2013) 214107.
[19] T. Maiti, R. Guo, and A. S. Bhalla, Ferroelectrics, 425 (2011) p4–26.
[20] C. Ostos , L. Mestres , M. L. Martı´nez-Sarrio´n , J. E. Garcı´a , A. Albareda , R. Perez Solid State Sciences 11 (2009) 1016–1022.
[21] S M Kaczmarek, M Or_owski, T Skibi_cki, A Jasik and L I Ivleva, Rev. Adv. Mater. Sci. 23 (2010) 80-87
[22] B Tilak, American Journal of Materials Science 2(4) (2012) p110-118.
[23] S. B. Kulkarni, S. S. Veer, D. J. Salukhe, S. R Kokare, P. B. Joshi , Indian Journal of Engineering and Material Science 15 (2008) p116-120.
[24] M. Shi , J. Zhong, R. Zuo, Y. Xu, L. Wang, H. Su, C Gu, Journal of Alloys and Compounds 562 (2013) 116–122.
[25] J. L. Zhang, P. F. Ji, Y. Q. Wu, X. Zhao, Y.Q. Tan, and C. L. Wang , Applied Physics Letters 104 (2014) 222909.

Author Profile

S. S. Mane received the B.Sc and M.Sc degree in Physics from Shivaji University, Kolhapur in 1983 & 1985. He is working as Associate Professor in Department of Physics, Karmaveer Bhaurao Patil Mahavidyalaya, Pandharpur, Solapur, 413304, India

Dr. D. J. Salunkhe received the B.Sc and M.Sc degree in Physics from Shivaji University, Kolhapur in 1982 & 1984. He received Ph.D. in Material Science from Shivaji University, Kolhapur in 2007. He worked as a Controller of Examinations, Solapur University, Solapur. He is working as Associate Professor in Department of Physics, Karmaveer Bhaurao Patil Mahavidyalaya, Pandharpur, Solapur, 413304, India.